sciendo

PRODUCTION ENGINEERING ARCHIVES 2021, 27(4), 242-247

PRODUCTION ENGINEERING ARCHIVES

ISSN 2353-5156 (print)
ISSN 2353-7779 (online)

Exist since 4th quarter 2013
Available online at https://pea-journal.eu

Stress-strain state of damaged reinforced concrete bended elements at operational load level

Nadiia Kopiika[1], Pavlo Vegera[1,*], Rostyslav Vashkevych[1], Zinoviy Blikharskyy[2]

[1] Lviv Polytechnic National University, 12 st. S. Bandera, Lviv, 79013, Ukraine; kopijka.nadija.1999@gmail.com (N.K.); rostyslav.v.vashkevych@lpnu.ua (R.V.);
[2] Czestochowa University of Technology, 69 st. Dabrowskiego, 42-201 Czestochowa, Poland; zinoviy.blikharskyy@pcz.pl
*Correspondence: pavlo.i.vehera@lpnu.ua

Article history
Received 22.05.2021
Accepted 13.08.2021
Available online 15.11.2021

Keywords
corrosion
steel rebar
real size beams
damaged beams

Abstract

Each structure is exposed to different influences during operation. As a result, there are various defects and damages of these elements that affect their safe operation. The article presents the results of experimental studies of reinforced concrete beams with damages to stretched reinforcement made with and without initial load application. As the damages were accepted one or five Ø5.6 mm holes. In one case, the damage was made until the beam destruction (up to the 8.4 mm opening) Control samples of both series were destroyed due to crushing of the compressed zone of concrete. Samples that were damaged without initial loading collapsed due to rupture of the stretched reinforcement. The same type of failure was identified for damages at the operational load level.

DOI: 10.30657/pea.2021.27.32 JEL: L70, L79

1. Introduction

Taking into consideration the prevalence of reinforced concrete structures in construction, the study of their load-bearing capacity changes during operation is the topical issue (Azizov et al., 2019; Karpiuk et al., 2019; Vatulia, 2018). The main issue in this area is the determination of bearing capacity, taking into account the damages` occurrence (Blikharskyy et al., 2021; Klymenko et al., 2020; Kotes et al., 2018). The most dangerous and common are damages in the compressed zone of concrete (Yogalakshmi et al., 2020). In the article (Lobodanov et al., 2021), the work of damaged reinforced concrete structures is investigated and calculation of such structures is given. The reduction of compressed elements cross-sectional area is more dangerous and important (Khmil et al., 2021b; Klymenko et al., 2019; Kochkarev et al., 2020). In such cases the damage does not only lead to load-bearing capacity decrease, but can also cause changes in the structure stress-strain state (for example, the transition from compressed to compressed-bended state of element due to damage). The study of steel corrosion for damaged RC constructions (Blikharskyy et al., 2020; Fomin et al., 2021). In the study (Lipinski, 2017), an attempt was made to analyze the effect of 20% aqueous NaCl solution on the stiffness of steel as the result of corrosion. Steel stiffness and corrosion wear were determined according to the corrosion time.

An important issue is the determination of actual bearing capacity of inclined sections in bended reinforced concrete elements (Kramarchuk et al., 2021; Pavlikov et al., 2019). Their complex stress-strain state and simplified calculations can lead to depletion of bearing capacity, especially in cases of existing damages in the support zones.

Studies of the stress - strain state are important taking into consideration the necessity of such structures` further restoration or strengthening (Kotes et al., 2020; Vatulia et al., 2017). Strengthening and restoration of structural reinforcement is always carried out taking into account its real stress-strain state. As the result, is obtained the structure that has worked in different stages, with different stresses in structural layers (at initial stages), which leads to another important issue, namely the reliability of such structures (Khmil et al., 2021a).

Particular attention should be paid to the establishment of residual load-bearing capacity of structures in which new materials are proposed (for example, composite (Turba and Solodkyy, 2021; Vavrus and Kotes, 2019)), as well as for structures with complex stress-strain state (such as pre-stressed structures (Bobalo et al., 2021)).

The study of the residual bearing capacity of elements and structures is the topical issue not only in construction but also in other fields of science and technology (Ulewicz R. and Ulewicz M., 2020; Czajkowska and Ingaldi, 2019), which only emphasizes the relevance of this issue.

2. Test program

The total number of tested beams was equal to 12. The samples were divided into two series: two samples of the 1st series and ten samples of the 2nd series. Thee test samples had the rectangular cross-section with dimensions equal to 200×100 mm and length of 2100 mm. Samples of 1st and 2nd series had the same geometric dimensions with deviation less than 2%. For the samples of 1st series the working reinforcement was made of 1Ø16 A 500S and 1Ø20 A500S – for the samples of 2nd series.

Compressed and transverse reinforcement is made of wire reinforcement of Ø5B500 and is identical for samples of both series. Reinforced concrete beams were made of concrete of C30/35 class.

All test samples were marked in following way: BC - control beam, or BD - damaged beam; the first digit is the series number, the second digit is the test sample number. For example, BC 1.2 means that the second control beam from the 1st series was tested. An index of 0.5 indicates the level at which the damage was made as the fraction from the received destructive. For conventional beams the notation * means that the test beam has five identical holes in the stretched reinforcement. The letter index "pd" (pointed damage) indicates damage with 5.6 mm hole, which corresponds to the decrease in the cross-sectional area of reinforcement from Ø20 to Ø16. The index "fd" (full damaged) means that the beams were damaged until the load-bearing capacity is exhausted due to the maximum reduction of cross-sectional area.

Reinforced concrete beams were tested according to the program given in Table 1.

The experimental study was performed by applying a static load as two concentrated forces. Two samples from the 1st and 2nd series were tested as control samples (without damages). The next two samples from the 2nd series were tested as follows:

- damages were performed by drilling one hole of Ø3 mm. After that the diameter of the hole was increased by 0.5 mm up to Ø5.6 mm. At such damage the residual diameter of armature corresponds to Ø16 mm;
- gradually, according to the research method from (Blikharskyy et al., 2020), the samples were brought to physical destruction.

The other 4 samples were tested in the following sequence:

- samples were loaded up to load level of 0.5 from the expected destructive value;
- the Ø3 mm hole was drilled, its diameter was gradually increased in increments of 0.5 mm. up to a value of 5.6 mm;
- gradually, according to the research method in (Blikharskyy et al., 2020), the samples were brought to physical destruction.

The last two samples were tested in the following sequence:

- samples were loaded up to the load level of 0.5 from the expected destructive value;
- the Ø3 mm hole was drilled, its diameter was gradually increased in increments of 0.5 mm until the load-bearing capacity of the sample is exhausted.

Table 1. Program of the experiment

№	Test beam marking	Concrete class	Working reinforcement	Test sample description
1.	BC 1.1	C30/35	1Ø16 A500S	Control samples (without damages)
2.	BC 1.2			
3.	BC 2.3		1Ø20 A500S	Control samples (without damages)
4.	BC 2.4			
5.	BD 2.5-0.0pd			Samples with one Ø5.6 mm hole in stretched reinforcement without initial load applied
6.	BD 2.6-0.0pd			
7.	BD 2.7-0.5pd			Samples with one Ø5.6 mm hole in stretched reinforcement at initial load level of 0.5
8.	BD 2.8-0.5pd			
9.	BD 2.9-0.5pd*			Samples with five Ø5.6 mm hole in stretched reinforcement at initial load level of 0.5
10.	BD 2.10-0.5pd*			
11.	BD 2.11-0.5fd			Samples with one hole in stretched reinforcement until the element is destroyed
12.	BD 2.12-0.5fd			

At each stage, after increasing the diameter of the hole the readings were recorded from the devices located as shown in study (Bobalo et al., 2021).

3. Experimental researching

The test specimens were tested by static load application, which was applied until the physical destruction occurred.

Control samples of the 1st and 2nd series were destroyed due to crushing of the compressed zone concrete in the central part of the beam. Damaged specimens, regardless of whether they were damaged during loading or not, were destroyed due to the stretched reinforcement rupture. It was identified that the bearing capacity of the samples varied depending on the damage type and the load level at which the damage occurred (see Table 2).

In the samples BD 2.5-0.0pd and BD 2.6-0.0pd, BC 1.1 and BC 1.2 the area of working reinforcement, as well as all other parameters (concrete strength, location of frames, etc.) were the same. However, according to Table. 2, the strength of samples with damaged reinforcement with 20 mm diameter (BD 2.5-0.0pd and BD 2.5-0.0pd) is greater than the strength of samples with working reinforcement of 16 mm diameter (BC 1.1 and BC 1.2). This could be explained by the fact that in

damaged samples the main working cross section of the reinforcement is the thermally strengthened outer layer. Therefore, the deviation of bearing capacity in damaged samples was at average 24%, whereas in undamaged samples with the same area of working reinforcement deviation was at average 31%. Significantly lower bearing capacity was identified for samples BC 1.1 and BC 1.2 with working reinforcement with 16 mm diameter in comparison with beams reinforced with 20 mm diameter rebar, the deviation was equal to 30.2%. In the samples damaged at load levels, the bearing capacity was approximately the same within 3.7… 13.2%. The higher bearing capacity of damaged specimens at load levels with damaged reinforcement of 20 mm diameter (the area of the damaged rebar corresponds to the area of 16 mm diameter) in comparison with samples with working 16 mm rebar could be explained by the presence of thermally strengthened layer.

Table 2. Strength of experimental samples damaged at load level

Sample marking	Load-bearing capacity exhaustion, kNm		Physical destruction, kNm		Deviation of load-bearing capacity compared to BC-1		Deviation of physical destruction compared to BC-1	
	Of sample	Average	Of sample	Average	Of sample	Average	Of sample	Average
BC 1.1	24.9	24.2	32.9	31.1	-	-	-	-
BC 1.2	23.5		29.3		-		-	
BC 2.3	16.3	16.9	20	21.1	32.6	30.2	35.7	32.2
BC 2.4	17.5		22.2		27.7		28.6	
BD 2.5-0.0pd	19	18.1	22.9	23.5	21.5	25.2	26.4	24.4
BD 2.6-0.0pd	17.2		24.1		28.9		22.5	
BD 2.7-0.5pd	23.3	21.5	26.9	25.5	3.7	11.2	13.5	18.0
BD 2.8-0.5pd	19.7		24.1		18.6		22.5	
BD 2.9-0.5pd*	17.5	18.4	21.9	23.5	27.7	24.0	29.6	24.4
BD 2.10-0.5pd*	19.3		25.1		20.2		19.3	
BD 2.11-0.5fd	15.0	15.0	15.0	15.0	39.8	37.8	54.4	48.2
BD 2.12-0.5fd	15.0		15.0		36.1		48.8	

Namely, due to the damage, the cross-sectional area of the core (cross-section of unstrengthened part of rebar) is significantly reduced, whereas the outer thermally-reinforced layer is slightly reduced; this fact explains the higher bearing capacity results. The number of holes also affects the bearing capacity of such samples. Thus, the samples BD 2.9-0.5pd* and BD 2.10-0.5pd* had larger number of holes (5 holes compared to other samples with 1 hole), which reduced the load-bearing capacity and, accordingly, increased the deviation compared to the control undamaged samples with working 20 mm steel bars up to 24.0%. When the samples are damaged at the operational load level, the load-bearing capacity is decreased due to reduction of working rebar cross section by 35% from the initial value. However, for samples, damaged at a load level of 0.5 from the expected destructive for control samples, the load-bearing capacity was 50% from bearing capacity, which is equal to the level of damaging.

4. Results and Discussion

The deformation specifics of compressed concrete and stretched working reinforcement of undamaged control samples with working reinforcement Ø20 mm (BC 2.3 and BC 2.4) are shown in Fig. 1. It should be noted that the graphs on Fig. 1 and others show the average values of both deformations and bending moments of the twin-beams.

As can be seen from Fig. 1, the deformations of the stretched reinforcement and concrete of the most compressed fiber increased gradually with the same growth of increasing load. When deformations in the stretched reinforcement reached the yield strength $\sigma_y = f_y$ at the load level of $M_{s,y}$=24.2 kNm, the bearing capacity of the samples was exhausted due to yield of the working reinforcement; accordingly, sharp increase in deformations of compressed concrete and stretched reinforcement is observed. The maximum deformations in the stretched reinforcement equal to $\varepsilon_{s,max}$=388·10-5 and in the most compressed fiber concrete equal to $\varepsilon_{c,max} = 309 \cdot 10^{-5}$ at the bending moment of M = 27.1 kNm were recorded. After that, when the ultimate deformations of concrete were reached, the brittle fracture of the most compressed concrete fiber under load M_{ult} = 31.1 kNm occurred.

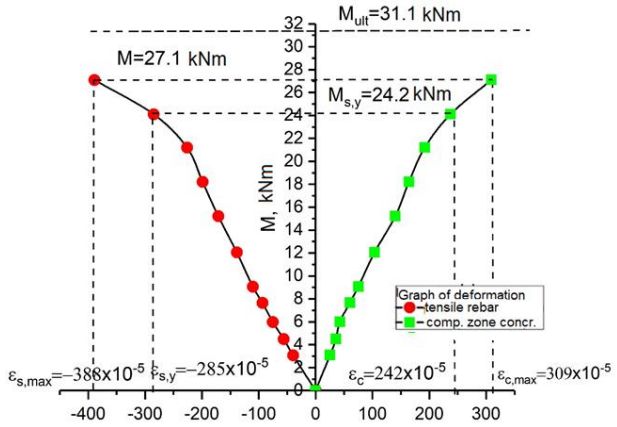

Fig. 1. The average deformation graphs of stretched reinforcement (left) and compressed concrete (right) of undamaged beams BC 2.3 and BC 2.4

In the samples BD 2.5-0.0pd and BD 2.6-0.0pd with working reinforcement of 20 mm without applying a load the 5.6 mm-diameter hole was made in working rebar, which led to reduction of the cross-sectional area to diameter of 16 mm. However, the hole reduces the cross-section of the core of the reinforcement, while leaving a larger part of thermally strengthened cross-sectional area. As a result, no clear region of yielding could be identified, which is shown by the results of sample beams BD 2.5-0.0pd and BD 2.6-0.0pd (Fig. 2). Gradual increase in the deformation of the stretched reinforcement and concrete of the most compressed fiber could be identified. Exhaustion of bearing capacity occurred at the moment $M_{s,y}$ = 24.2 kNm, when the deformation of the stretched reinforcement achieved the beginning of yielding $\varepsilon_{s,y} = 285 \cdot 10^{-5}$.

The maximum values of deformation of the most compressed concrete fiber $\varepsilon_{c,\,max} = 195 \cdot 10^{-5}$ and of stretched reinforcement $\varepsilon_{s,max}=329 \cdot 10^{-5}$ were recorded at the moment M = 19 kNm.

After reaching the moment M_{ult}=23.5 kNm, the samples were physically destroyed due to the rupture of the stretched working reinforcement.

It is important to note the destruction specifics of the samples, which is the result of damage of much larger part of the unstrengthened layer of reinforcement and minor thermally strengthened layer reduction.

In addition, no destruction of the compressed zone concrete occurred and no achievement of limit values for the most compressed concrete fibers was identified. The destruction occurred due to the rupture of the working rebar. This could be explained by the fact that the damage of the stretched reinforcement has the local character in one place, which corresponds to the drilled hole.

When testing control samples with working reinforcement with a diameter of 16 mm, the gradual increase in deformations of stretched reinforcement and concrete of the most compressed fiber is observed (Fig. 3). At loading of $M_{s,y}$=16.9 kNm deformations of the stretched armature were equal to $\varepsilon_{s,y}=285 \cdot 10^{-5}$, which corresponds to the beginning of yielding and accordingly exhaustion of bearing capacity are reached. After achieving these deformations, there is the sharp increase in the deformations of the compressed and stretched zone.

Samples BD-2.7-0.5pd and BD-2.8-0.5pd were damaged according to the above indicated procedure at a load level of 50% of the bearing capacity of the control undamaged samples. The bending moment at which the damage was performed corresponded to M =16.3 kNm. Deformations of the working stretched reinforcement and concrete of the most compressed fiber increased smoothly and had the linear character (Fig. 4).

During the gradual damage of the working reinforcement by drilled holes of increasing diameters at bending moment M = 16.3 kNm deformations increased at a constant load level. With growth of load higher than M = 16.3 kNm in the beams and with reduced working rebar area due to damage, more intense increase in deformation was identified. The deformations of the reinforcement reached the beginning of the yield strength and, accordingly, the samples reached the depletion of the bearing capacity for the yield of the reinforcement at $M_{s,y}$ = 21.5 kNm. The maximum deformations were recorded at load of M = 22.5 kNm, which for stretched working reinforcement were equal to $\varepsilon_{s,max}=316 \cdot 10^{-5}$. The largest deformations for the most compressed fiber concrete were equal to $\varepsilon_{c,max}=234 \cdot 10^{-5}$.

When the bending moment M = 25.5 kNm was reached, physical failure occurred due to rupture of the working reinforcement.

Similarly, to the case of working reinforcement damage for the deformation of concrete of the most compressed fiber and stretched reinforcement, the uniform increase of linear nature is observed (Fig. 5). At the bending moment M = 16.3 kNm was performed damage of the stretched working reinforcement. For samples with damages was identified an increase in the deformation of the working reinforcement and concrete of the most compressed fiber at constant load level.

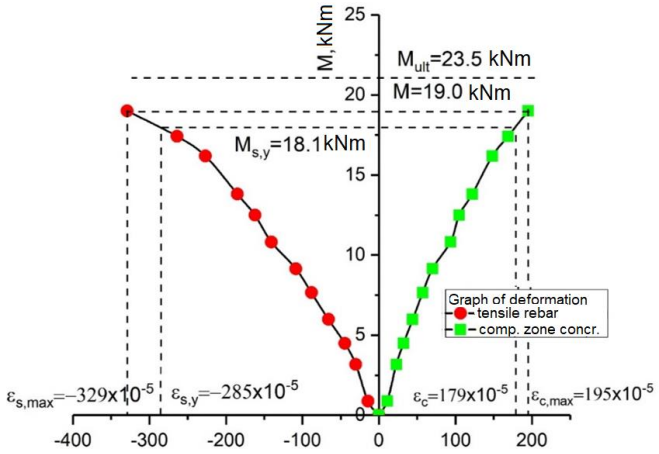

Fig. 2. The average deformation graphs of stretched reinforcement (left) and compressed concrete (right) of damaged beams BD 2.5-0.0pd and BD 2.6-0.0pd

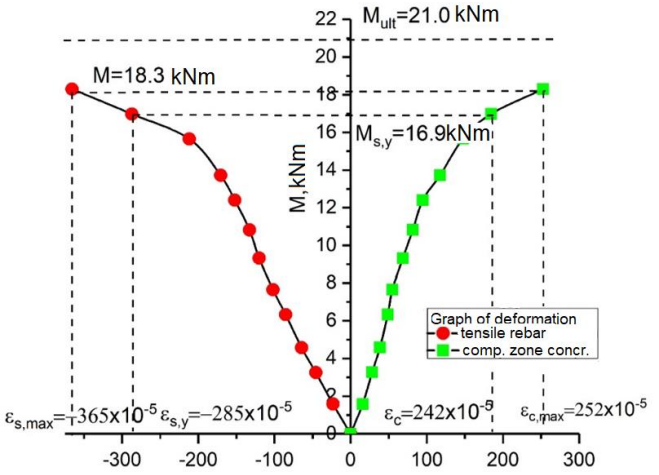

Fig. 3. Average deformation graphs of stretched reinforcement (left) and compressed concrete (right) of undamaged beams BC 1.1 and BC 1.2

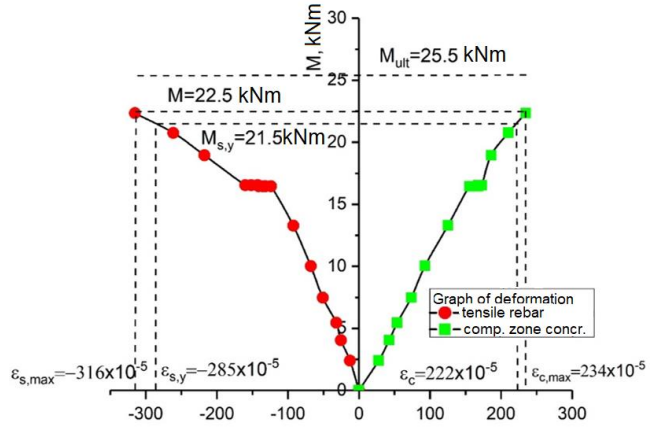

Fig. 4. Average deformation graphs of stretched reinforcement (left) and compressed concrete (right) of undamaged beams of the 1st series BD-2.7-0.5pd and BD-2.8-0.5pd

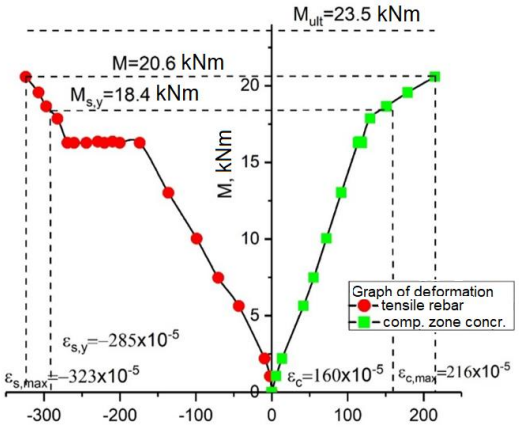

Fig. 5. The average deformation graphs of stretched reinforcement (left) and compressed concrete (right) of damaged beams BD-2.9-0.5pd* and BD-2.10-0.5pd*

After reduction of the reinforcement cross section by 36% (the cross-sectional area reduction which corresponded to working rebar of 16 mm diameter), similarly, the linear increase in deformation is observed. When the rebar deformations reached the yielding at the bending moment $M_{s,y}$ = 18.4 kNm, the bearing capacity of the samples was exhausted due to the working reinforcement yielding.

Control samples BC 2.3 and BC 2.4 showed the bearing capacity higher by 30.2% compared to samples of the 1st series. Samples damaged without the initial level of load showed the bearing capacity quite close to the samples of the 1st series. Therefore, the damage simulated the reduction of the reinforcement diameter from Ø20 to Ø16 quite accurately. At the load level of 0.5 of the expected destructive of control samples, the load-bearing capacity of the specimens damaged by points (with one hole) is higher by 11%. Accordingly, for the case of the damages along the length (by 5 holes) the increase of load-bearing capacity is 24% higher. Therefore, the load level affects the load-bearing capacity of the samples that are damaged.

5. Conclusion

1. The level of load and damage specifics (point or distributed) affect the depletion of bearing capacity, namely:
- in the case of point damages, the bearing capacity of samples is higher by 11% (in comparison with similar undamaged samples);
- in the case of damages along on sample length bearing capacity is higher by 24% in comparison with control samples.

2. Reinforced concrete beams with working reinforcement of ø20, the area of which was decreased by damage to the area analogous to the ø16 rebar had a final bearing capacity higher than reinforced concrete beams reinforced with ø16 rebar without damage. This could be explained by the fact that the damage of the ø20 rebar by drilling holes, in the greater extent the core with smaller physical and mechanical properties was damaged, whereas the outer thermally strengthened layer with higher physical and mechanical properties was damaged to a lesser extent.

3. Analysis of the results shows that in the case of damaged thermally-strengthened reinforcement, it is necessary to take into account the presence of an outer thermally strengthened layer within the rebar cross section, which has higher physical and mechanical characteristics, as well as the presence of inner core with lower physical and mechanical characteristics. With partial or complete damage of the outer thermally strengthened layer of steel bars, their physical and mechanical characteristics can be significantly reduced, which will affect the final load-bearing capacity of structures.

References

Azizov, T.N., Kochkarev, D.V., Galinska, T.A., 2019. New design concepts for strengthening of continuous reinforced-concrete beams. IOP Conference Series: Materials Science and Engineering, 708(1).

Blikharskyy, Y., Kopiika, N. and Selejdak, J., 2020. Non-uniform corrosion of steel rebar and its influence on reinforced concrete elements` reliability. Production Engineering Archives, 26(2), 67-72.

Blikharskyy, Y., Vashkevych, R., Kopiika, N., Bobalo, T., Blikharskyy, Z., 2021. Calculation residual strength of reinforced concrete beams with damages, which occurred during loading. IOP Conference Series: Materials Science and Engineering,1021(1).

Bobalo, T., Blikharskyy, Y., Kopiika, N., Volynets, M., 2021. Influence of the Percentage of Reinforcement on the Compressive Forces Loss in Prestressed RC Beams Strengthened with a Package of Steel Bars. Lecture Notes in Civil Engineering, 100, 53-62.

Czajkowska, A., Ingaldi, M., 2019. Analysis of the impact of individual phases in the building process cycle on the environment with respect to the principles of sustainable development. IOP Conference Series: Earth and Environmental Science, 214(1), 012012. DOI: 10.1088/1755-1315/214/1/012012

Fomin, O., Vatulia, G., Horbunov, M., Lovska, A., Píštěk, V., Kučera, P., 2021. Determination of residual resource of flat wagons load-bearing structures with a 25-year service life. IOP Conference Series: Materials Science and Engineering, 1021(10).

Karpiuk, V., Somina, Y., Maistrenko, O., 2019. Engineering Method of Calculation of Beam Structures Inclined Sections Based on the Fatigue Fracture Model. Lecture Notes in Civil Engineering, 47, 135-144.

Khmil, R.Y., Tytarenko, R.Y., Blikharskyy, Y.Z., Vegera, P.I., 2021a. Improvement of the method of probability evaluation of the failure-free operation of reinforced concrete beams strengthened under load. IOP Conference Series: Materials Science and Engineering, 1021(1).

Khmil, R., Tytarenko, R., Blikharskyy, Y., Vegera, P., 2021b. The Probabilistic Calculation Model of RC Beams, Strengthened by RC Jacket. Lecture Notes in Civil Engineering, 100, 182-191.

Klymenko, Y., Grynyova, I., Kos, Z., 2019. The method of calculating the bearing capacity of compressed stone pillars. Lecture Notes in Civil Engineering, 47, 161-167.

Klymenko, Y., Kos, Z., Grynyova, I., Maksiuta, O., 2020. Operation of Damaged H-Shaped Columns. Lecture Notes in Civil Engineering, 100, 192-201.

Kochkarev, D., Azizov, T., Galinska, T., 2020. Design of Effective Statically Indeterminate Reinforced Concrete Beams. Lecture Notes in Civil Engineering, 73, 83-93, DOI: 10.1007/978-3-030-42939-3_10

Kotes, P., Strieska, M., Brodnan, M., 2018. Sensitive analysis of calculation of corrosion rate according to standard approach. IOP Conference Series: Materials Science and Engineering, 385(1), 012031, DOI: 10.1088/1757-899X/385/1/012031

Koteš, P., Vavruš, M., Jošt, J., Prokop, J., 2020. Strengthening of concrete column by using the wrapper layer of fibre reinforced concrete. Materials, 12(23), 1-21, DOI: 10.3390/ma13235432

Kramarchuk, A., Ilnytskyy, B., Bobalo, T., Lytvyniak, O., (2021). A study of bearing capacity of reinforced masonry beams with GFRP reinforcement. IOP Conference Series: Materials Science and Engineering, 1021(1).

Lipiński, T., 2017. Roughness of 1.0721 steel after corrosion tests in 20% NaCl. Production Engineering Archives, 15(15), 27-30.

Lobodanov, M., Vegera, P., Khmil, R., Blikharskyy, Z., 2021. Influence of Damages in the Compressed Zone on Bearing Capacity of Reinforced Concrete Beams. Lecture Notes in Civil Engineering, 100, 260-267.
Pavlikov, A., Kochkarev, D., Harkava, O., 2019. Calculation of reinforced concrete members strength by new concept. Proceedings of the fib Symposium 2019, Concrete - Innovations in Materials, Design and Structures, 820-827.
Turba, Y., Solodkyy, S., 2021. Crack Resistance of Concretes Reinforced with Polypropylene Fiber. Lecture Notes in Civil Engineering, 100, 474-481, DOI: 10.1007/978-3-030-57340-9_58
Ulewicz, R., Ulewicz, M., 2020. Problems in the Implementation of the Lean Concept in the Construction Industries. Lecture Notes in Civil Engineering, 47, 495-500, DOI: 10.1007/978-3-030-27011-7_63
Vatulia, G., Lobiak, A., Orel, Y., 2017. Simulation of performance of circular CFST columns under short-time and long-time load. Matec Web of Conferences, 116, 02036, DOI: 10.1051/matecconf/201711602036
Vatulia, G., Rezunenko, M., Petrenko, D., Rezunenko, S., 2018. Evaluation of the carrying capacity of rectangular steel-concrete columns. Civil and Environmental Engineering, 14(1), 76-83. DOI: 10.2478/cee-2018-0010
Vavruš, M., Koteš, P., 2019. Numerical comparison of concrete columns strengthened with layer of fiber concrete and reinforced concrete. Transportation Research Procedia, 40, 920-926.
Yogalakshmi, N.J., Rao, K.B., Anoop, M.B., 2020. Durability-Based Service Life Design of RC Structures—Chloride-Induced Corrosion. Reliability, Safety and Hazard Assessment for Risk-Based Technologies, Springer, Singapore, 579-590, DOI: 10.1007/978-981-13-9008-1_48.

运行荷载水平下受损钢筋混凝土弯曲元件的应力应变状态

關鍵詞
腐蚀
钢筋
实际尺寸梁
损坏的梁

摘要
每个结构在运行过程中都会受到不同的影响。 因此，这些元件存在各种缺陷和损坏，影响其安全运行。 本文介绍了在施加和不施加初始载荷的情况下对拉伸钢筋造成损坏的钢筋混凝土梁的实验研究结果。 由于损坏可接受一或五个 Ø5.6 毫米孔。 在一种情况下，损坏一直持续到梁破坏（高达 8.4 毫米的开口）两个系列的对照样品都因混凝土压缩区的压碎而被破坏。由于拉伸钢筋破裂，在没有初始加载的情况下损坏的样品倒塌。 相同类型的故障被确定为在操作负载水平上的损坏。